Two-Mode Thermal-Noise Squeezing in an Electromechanical Resonator

I. Mahboob,* H. Okamoto, K. Onomitsu, and H. Yamaguchi
NTT Basic Research Laboratories, NTT Corporation, Atsugi-shi, Kanagawa 243-0198, Japan
(Received 6 June 2014; published 17 October 2014)

An electromechanical resonator is developed in which mechanical nonlinearities can be dynamically engineered to emulate the nondegenerate parametric down-conversion interaction. In this configuration, phonons are simultaneously generated in pairs in two macroscopic vibration modes, resulting in the amplification of their motion. In parallel, two-mode thermal squeezed states are also created, which exhibit fluctuations below the thermal motion of their constituent modes as well as harboring correlations between the modes that become almost perfect as their amplification is increased. The existence of correlations between two massive phonon ensembles paves the way towards an entangled macroscopic mechanical system at the single phonon level.

DOI: 10.1103/PhysRevLett.113.167203 PACS numbers: 85.85.+j, 05.45.-a, 42.65.Es, 42.65.Lm

Two-mode vacuum squeezed states pioneered in quantum optics offer a highly versatile resource for nonclassical light, where entangled photon pairs are generated from parametric down-conversion in a nonlinear media [1–5]. Indeed, the success of two-mode squeezing has even inspired a reinterpretation of this concept with microwave photons by exploiting the Josephson nonlinearity in superconducting circuits [6–10]. Perhaps the most striking iteration of this phenomenon can be found in hybrid systems composed of a mechanically compliant element that is parametrically coupled to an electromagnetic resonator [11]. These so-called cavity electro- or

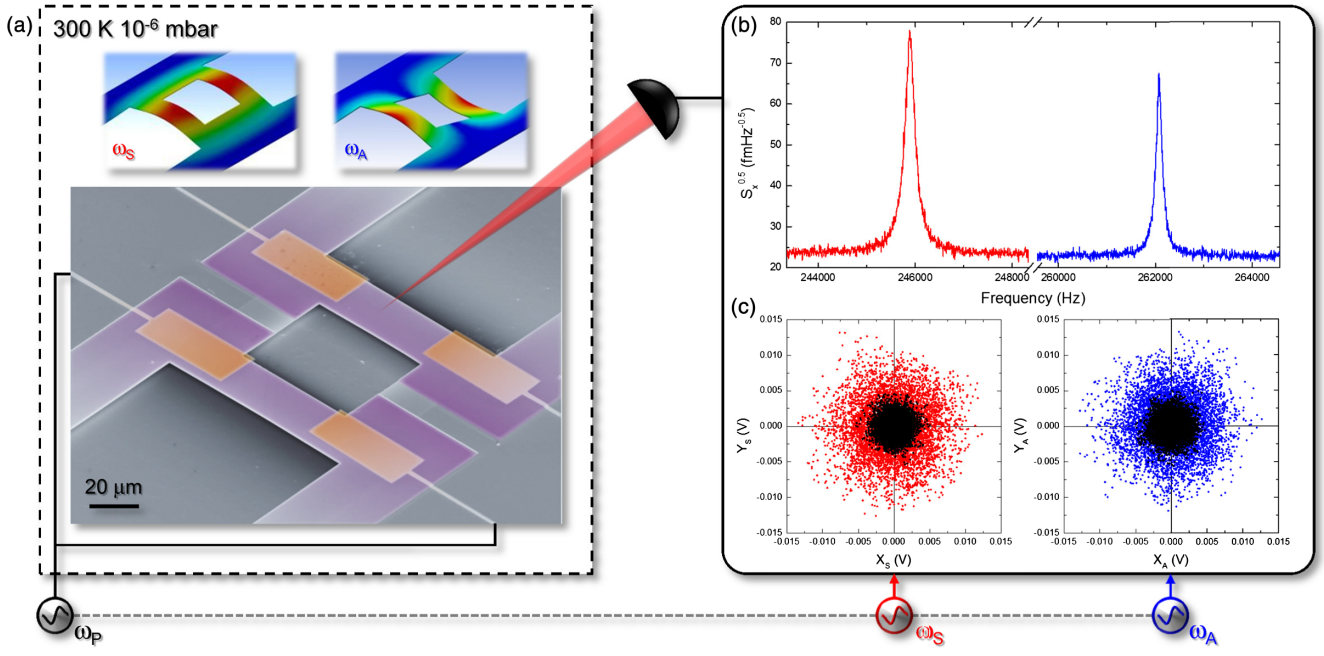

FIG. 1 (color online). (a) An electron micrograph of the GaAs based coupled electromechanical resonators incorporating a buried Si-doped layer that is confined within a shallow mesa (purple) where the mechanical elements are integrated with Au Schottky gates (orange) to form the piezoelectric transducers [22]. The vibration of the modes is detected via the partially depicted laser interferometer from the right beam, i.e., not the center of mass with the parametric down-conversion being piezoelectrically activated by applying a pump voltage to both electrodes on the left beam [22]. The pumping generator (ω_P) and the local oscillators (ω_S and ω_A) are all continuously synchronized (gray dashed line) to ensure phase locked measurements. Also shown are the vibration profiles for the symmetric and asymmetric modes extracted from a finite element analysis. (b) The output noise from the interferometer, measured in a spectrum analyzer, reveals the two modes via their picometer order thermal vibrations. (c) The on-resonance thermal motion of both modes projected in phase space. Also shown is the electrical noise in the measurement setup (black points) acquired in an off-resonance configuration [22].

optomechanical systems can readily host parametric down-conversion, which not only amplifies both resonators [12] but at the single phonon and photon level can generate an entanglement between two vastly dissimilar systems [13]. Tantalizingly, an all-mechanical variant of this interaction would not only open up a path towards the generation of a macroscopic mechanical entanglement [14,15] but would also offer the unique prospect of decoding the nature of its absence in our everyday classical world [16].

One intuitive approach to mechanical two-mode squeezing is to utilize multimode electromechanical resonators, which can mimic the dynamics of cavity electro- or optomechanical systems [17–20]. Although these phonon cavity electromechanical systems can host parametric down-conversion, in practice, the large input excitation needed to activate the nonlinear parametric interaction between two vibration modes has yielded only modest gains, which has rendered the study of this interaction inaccessible [17,18]. To address this, we have developed an electromechanical resonator, shown in Fig. 1(a) and detailed elsewhere, that consists of two doubly clamped beams that are spectrally closely spaced and intercoupled via an exaggerated overhang between them [21]. This structure sustains two strongly coupled vibration modes labeled symmetric (S) and asymmetric (A), also shown in Fig. 1(a), and in combination with piezoelectric transducers that are incorporated directly into the mechanical elements provides the key to realizing efficient parametric down-conversion.

The piezoelectric transducers offer potent means to nonlinearly modulate the spring constant of the electromechanical system by generating stress [18,19]. If this modulation is activated at the frequency difference between the modes, it enables a beam splitter interaction to be switched on, which results in sidebands being generated around both modes, and their subsequent overlap enables them to couple and exchange energy [18,19,23,24]. On the other hand, if this modulation is implemented at the sum frequency of the two modes, it can permit parametric down-conversion of the input modulation, resulting in nondegenerate parametric amplification of both modes [12,18]. Physically, the sum frequency modulation of the electromechanical system's spring constant has components that can parametrically activate the symmetric and asymmetric modes.

The total Hamiltonian of the system in this configuration can then be expressed as

$$H = \sum_{n=S}^{A} (P_n^2/2m_n + m_n\omega_n^2 Q_n^2/2) + \Lambda Q_S Q_A \cos(\omega_P t), \quad (1)$$

where the first two terms are the kinetic and potential energies, respectively, with canonical coordinates Q_n and P_n denoting the position and conjugate momentum of the constituent modes with frequencies ω_n and mass m_n [18]. The last term describes the parametric down-conversion when the modulation is activated at the sum frequency $\omega_P = \omega_S + \omega_A$, where the coupling coefficient Λ is proportional to the pump voltage as detailed in the Supplemental Material [22]. Although the present formulation is manifestly classical, the last term is analogous to $a_S a_A + a_S^\dagger a_A^\dagger$ in a quantum mechanical picture within the rotating frame approximation, where a_n and $a_n^\dagger$ are the annihilation and creation operators for the two modes, and this interaction forms the basis of two-mode squeezing, i.e., entanglement generation from parametric down-conversion [1,25]. Ostensibly, entanglement between the two modes is unavailable in the present classically bound system, but remarkably this Hamiltonian indicates that correlations between the modes can even emerge in the thermal limit with large phonon populations [22]. Consequently, an observation of the correlations generated by the parametric down-conversion process, between two classical modes, would lay a pivotal marker on the road towards entangling two massive mechanical systems [14].

The vibration of the two modes can be readily resolved via their thermal motion in the output noise spectrum from an optical interferometer based probe, which reveals

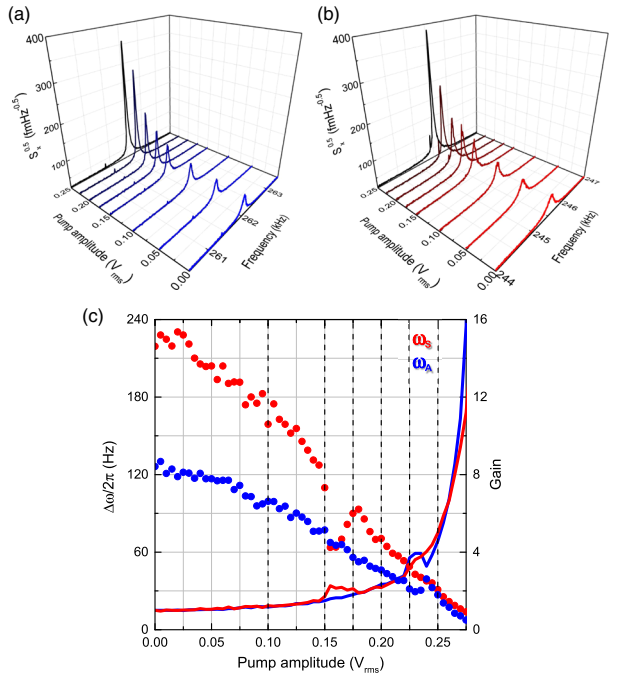

FIG. 2 (color online). (a),(b) The thermal motion of the symmetric and asymmetric modes, respectively, is amplified when the electromechanical resonator's spring constant is pumped at the sum frequency of the constituent modes. (c) The resultant gain of both modes referenced to their bare thermal motion (solid lines) is accompanied with a narrowing of their respective power bandwidths $\Delta\omega/2\pi$ (points) as a function of the pump intensity. At the largest pump amplitudes, the quality factor of both modes converges to $\sim 10^5$ before undergoing nondegenerate parametric resonance.

$\omega_S/2\pi = 246$ kHz and $\omega_A/2\pi = 262$ kHz with quality factors of 1300 and 2200, respectively, as shown in Fig. 1(b). Alternatively, the thermal motion from both modes can also be projected into phase space by decomposing their displacements $Q_n(t) = X_n \cos(\omega_n t) + Y_n \sin(\omega_n t)$ within a narrow bandwidth into in-phase and quadrature components, i.e., X_n and Y_n respectively. In practice this involves mixing the output from the interferometer with two local oscillators, which are locked exactly onto the resonances of the two modes, and then demodulated in two lock-in detectors over a period of 300 s with a sampling rate of 50 ms, resulting in four simultaneously acquired time series for all four components, each with 6000 points per measurement. The phase portraits reconstructed from this data yield circularly symmetric distributions, shown in Fig. 1(c), which confirm that the thermal motion of both modes is random with all vibration phases being equally available [26].

First, in order to investigate the availability of parametric amplification, namely the rate at which the phonons are generated begins to exceed their rate of decay from both modes, the system is pumped at ω_P by activating the piezoelectric transducers as detailed in Fig. 1(a) and the output noise spectra around both modes is acquired as shown in Figs. 2(a) and 2(b). This measurement reveals that the thermal motion of both modes can be amplified as the pump voltage is increased, with gains of more than 20 dB becoming available, before they undergo regenerative oscillations as shown in Fig. 2(c) [11,12,18,19]. Repeating this measurement and projecting the outputs in phase space, as detailed above and shown in Figs. 3(a) and 3(b), not only reconfirms the amplification but also indicates the phase preserving nature of this effect [6,7].

The parametric down-conversion simultaneously generates signal and idler phonons in both modes, thus amplifying their thermal motion. As a result, the noise, namely the amplified thermal motion of both modes, should be strongly correlated or, in other words, a two-mode thermal squeezed state will be generated [7]. In order to confirm this, the cross quadratures of the data shown in Figs. 3(a) and 3(b) are extracted; i.e., the in-phase component of the symmetric mode versus the quadrature component of the asymmetric mode and vice versa are plotted as shown in Figs. 3(c) and 3(d). This analysis unambiguously reveals two-mode thermal-noise squeezing, where the noise along one phase is deamplified at the expense of increased noise in the perpendicular phase, resulting in squeezed distributions. This specificity in phase space indicates that the two modes are

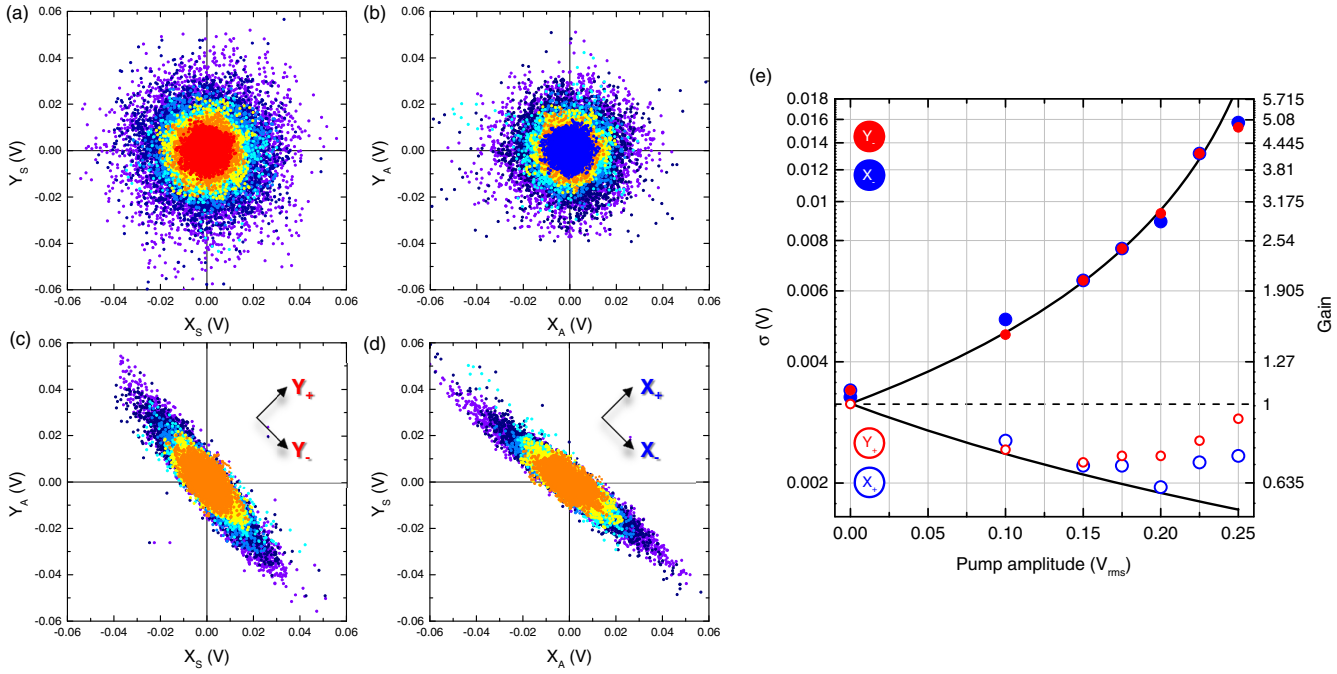

FIG. 3 (color online). (a),(b) The phase portraits of the symmetric and asymmetric modes exhibit phase-conserving nondegenerate parametric amplification in response to the pump phonons undergoing parametric down-conversion when their intensity is increased from 0 to 0.25 V_{rms} in increments detailed in panel (e). (c),(d) The cross quadratures of the above data take only specific values in phase space indicating the existence of correlations between the modes where the squeezing is enhanced as the pump intensity is increased. (e) The two-mode thermal squeezed states are quantified, in the rotated axis depicted in the insets to Figs. 3(c) and 3(d), via the standard deviations of their phase-space distributions (points) where the gain is calibrated with respect to the narrowest bare thermal distribution from Y_A (dashed line) and is consistent with the theoretical trends derived from the above Hamiltonian (solid lines) as detailed in the Supplemental Material [22]. Note that the uncertainties associated with the extracted standard deviations are 2 orders of magnitude smaller and cannot be shown [22].

correlated whereas an absence of any correlations would plainly lead to circular distributions.

In order to quantify the noise in the two-mode thermal squeezed states, a phase factor is introduced to rotate and then project the amplified (squeezed) distributions onto the rotated in-phase (quadrature) axis, namely X_- and Y_- (X_+ and Y_+) as shown in Figs. 3(c) and 3(d), to statistically weigh their profiles [22]. This analysis reveals Gaussian distributions with zero mean for all components where the extracted standard deviations σ as a function of the pump amplitude enable a measure of the thermal fluctuations in the squeezed states as shown in Fig. 3(e) [22]. As expected, the amplification of the in-phase components results in larger standard deviations with the corresponding gains consistent with the noise spectra measurements detailed by the dashed lines in Fig. 2(c). Concurrently, the quadrature component distributions become narrower with their standard deviations becoming even less than that of the bare modes as referenced by the dashed line in Fig. 3(e). Calibrating this reduction with respect to the narrowest bare thermal distribution yields a conservative lower limit of −4.76 dB squeezing below the thermal level at 300 K [26–28], which is limited by pump induced heating as detailed in the Supplemental Material [22].

Although noise reduction in the squeezed states below the thermal level of the bare modes is one characteristic of their interdependence [8], further substantiating evidence can also be elicited by analyzing the temporal correlations in the data shown in Figs. 3(c) and 3(d). To that end the absolute correlation coefficient $|\mathrm{cov}(Z_i Z_j(\tau))/\sigma_{Z_i}\sigma_{Z_j}(\tau)|$, where the numerator describes the covariance, $Z_i \in \{X_S, Y_S, X_A, Y_A\}$, and τ is a delay between the constituent time series, is evaluated. The results of this analysis for a pump amplitude of 0.1 V_{rms}, shown in Fig. 4(a), reveal the absence of any correlation between X_S and Y_S, as attested to by their circular distribution in phase space [see Fig. 3(a)]. In contrast, the autocorrelation of X_S is exactly 1 at $\tau = 0$, confirming the perfect correlation expected in this configuration. However, finite correlations between $X_S : Y_A$ and $X_A : Y_S$ can also be discerned at $\tau = 0$, which indicates that the pump simultaneously generates signal and idler phonons in both modes in pairs, which is the signature feature of parametric down-conversion [29].

The correlation coefficients at $\tau = 0$ can be recast into a matrix for all permutations of Z_i, as shown in Fig. 4(b), which reveals, in addition to the expected perfect autocorrelations captured by the diagonal elements, finite valued off-diagonal elements that confirm the existence of correlations between the two modes. Naturally, the magnitude of the off-diagonal elements can be amplified as the pump intensity is increased as shown in Fig. 4(c) and this quantitatively confirms that the two mechanical vibration modes become almost perfectly entwined as their correlation coefficient tends to 1. The corresponding variation of the correlation coefficient can be reproduced by the parametric down-conversion Hamiltonian as shown in Fig. 4(c) and thus the simultaneous generation of phonons in both modes not only amplifies their thermal fluctuations but in the process fundamentally links them [22].

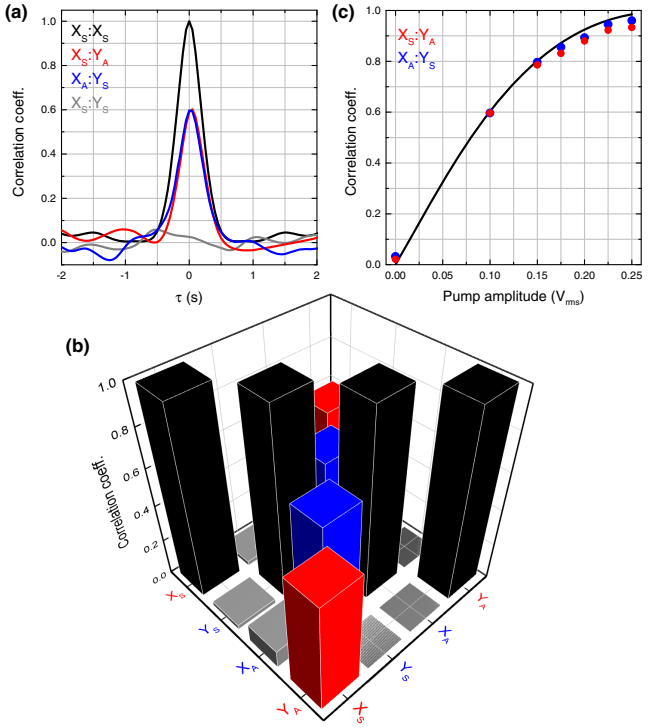

FIG. 4 (color online). (a) The absolute correlation coefficient between various combinations of components from both modes extracted with a pump amplitude of 0.1 V_{rms} as a function of delay time τ. (b) The corresponding correlation coefficient matrix at $\tau = 0$ reveals finite off-diagonal elements that verify the intertwined nature of the two-mode thermal squeezed states. (c) The variation of the off-diagonal elements of the correlation matrix as a function of pump intensity (points) and the corresponding theoretical response (solid line).

To evaluate the feasibility of generating two-mode vacuum squeezed states, the energy of the symmetric and asymmetric modes can be expressed in terms of their phonon number $N_n = k_B T/\hbar\omega_n$ where k_B is the Boltzmann constant and $\hbar$ is the reduced Plank constant, which reveals that both modes host 24–26 × 10^6 phonons at $T = 300$ K. Consequently, even if the present experiment could be operated at millikelvin temperatures, the symmetric and asymmetric modes would still sustain 1000 s of phonons where the −4.76 dB squeezing, approximately a factor of 2 reduction in the amplitude fluctuations corresponding to a factor of 4 reduction in the underlying phonon populations, would still preclude the generation of mechanical two-mode vacuum squeezed states. Indeed this analysis vividly illustrates the need for higher frequency mechanical modes in combination with cooling as necessary prerequisites to attaining $N_n < 1$ in order to explore two-mode vacuum squeezing [13].

The observation of correlations between two ensembles of millions of phonons, corresponding to the tangible motion of two massive mechanical vibration modes, opens up a new perspective on the study of correlated mechanical systems as well as heralding the prospect of quantum optics being translated to acoustics in mechanically compliant architectures [30,31]. Consequently, these results hail a landmark step on the journey towards generating an all-mechanical macroscopic entanglement as they establish that the nonlinear interaction at the heart of two-mode squeezing can be accessed in a purely mechanical system.

The authors are grateful to D. Hatanaka and N. Kitajima for support, and to N. Lambert, J. R. Johansson, and F. Nori for discussions and comments. This work was partly supported by JSPS KAKENHI Grant No. 23241046.

*imran.mahboob@lab.ntt.co.jp

[1] C. C. Gerry and P. L. Knight, *Introductory Quantum Optics* (Cambridge University Press, Cambridge, England, 2005).
[2] M. D. Reid and P. D. Drummond, Phys. Rev. Lett. **60**, 2731 (1988).
[3] Z. Y. Ou and L. Mandel, Phys. Rev. Lett. **61**, 50 (1988).
[4] Y. H. Shih and C. O. Alley, Phys. Rev. Lett. **61**, 2921 (1988).
[5] Z. Y. Ou, S. F. Pereira, H. J. Kimble, and K. C. Peng, Phys. Rev. Lett. **68**, 3663 (1992).
[6] N. Bergeal, F. Schackert, M. Metcalfe, R. Vijay, V. E. Manucharyan, L. Frunzio, D. E. Prober, R. J. Schoelkopf, S. M. Girvin, and M. H. Devoret, Nature (London) **465**, 64 (2010).
[7] C. Eichler, D. Bozyigit, C. Lang, M. Baur, L. Steffen, J. M. Fink, S. Filipp, and A. Wallraff, Phys. Rev. Lett. **107**, 113601 (2011).
[8] N. Bergeal, F. Schackert, L. Frunzio, and M. H. Devoret, Phys. Rev. Lett. **108**, 123902 (2012).
[9] E. Flurin, N. Roch, F. Mallet, M. H. Devoret, and B. Huard, Phys. Rev. Lett. **109**, 183901 (2012).
[10] E. Flurin, N. Roch, J. D. Pillet, F. Mallet, and B. Huard, arXiv:1401.5622.
[11] M. Aspelmeyer, T. J. Kippenberg, and F. Marquardt, arXiv:1303.0733v1.
[12] F. Massel, T. T. Heikkilä, J. M. Pirkkalainen, S. U. Cho, H. Saloniemi, P. J. Hakone, and M. A. Sillanpää, Nature (London) **480**, 351 (2011).
[13] T. A. Palomaki, J. D. Teufel, R. W. Simmonds, and K. W. Lehnert, Science **342**, 710 (2013).
[14] S. Mancini, V. Giovannetti, D. Vitali, and P. Tombesi, Phys. Rev. Lett. **88**, 120401 (2002).
[15] A. D. O'Connell, M. Hofheinz, M. Ansmann, R. C. Bialczak, M. Lenander, E. Lucero, M. Neeley, D. Sank, H. Wang, M. Weides *et al.*, Nature (London) **464**, 697 (2010).
[16] W. H. Zurek, Phys. Today **44**, No. 10, 36 (1991).
[17] W. Venstra, H. Westra, and H. van der Zant, Appl. Phys. Lett. **99**, 151904 (2011).
[18] I. Mahboob, K. Nishiguchi, H. Okamoto, and H. Yamaguchi, Nat. Phys. **8**, 387 (2012).
[19] H. Okamoto, A. Gourgout, C.-Y. Chang, K. Onomitsu, I. Mahboob, E. Y. Chang, and H. Yamaguchi, Nat. Phys. **9**, 480 (2013).
[20] T. Faust, J. Rieger, M. J. Seitner, J. P. Kotthaus, and E. M. Weig, Nat. Phys. **9**, 485 (2013).
[21] H. Okamoto, N. Kitajima, K. Onomitsu, R. Kometani, S. Warisawa, S. Ishihara, and H. Yamaguchi, Appl. Phys. Lett. **98**, 014103 (2011).
[22] See Supplemental Material at http://link.aps.org/supplemental/10.1103/PhysRevLett.113.167203 for experimental details, data analysis and modelling.
[23] J. D. Teufel, T. Donner, D. Li, J. W. Harlow, M. S. Allman, K. Cicak, A. J. Sirois, J. D. Whittaker, K. W. Lehnert, and R. W. Simmonds, Nature (London) **475**, 359 (2011).
[24] J. Chan, T. P. M. Alegre, A. H. Safavi-Naeini, J. T. Hill, A. Krause, S. Groeblacher, M. Aspelmeyer, and O. Painter, Nature (London) **478**, 89 (2011).
[25] S. G. Hofer, W. Wieczorek, M. Aspelmeyer, and K. Hammerer, Phys. Rev. A **84**, 052327 (2011).
[26] D. Rugar and P. Grütter, Phys. Rev. Lett. **67**, 699 (1991).
[27] J. Suh, M. D. LaHaye, P. M. Echternach, K. C. Schwab, and M. L. Roukes, Nano Lett. **10**, 3990 (2010).
[28] A. Szorkovszky, G. A. Brawley, A. C. Doherty, and W. P. Bowen, Phys. Rev. Lett. **110**, 184301 (2013).
[29] D. C. Burnham and D. L. Weinberg, Phys. Rev. Lett. **25**, 84 (1970).
[30] J. R. Johansson, N. Lambert, I. Mahboob, H. Yamaguchi, and F. Nori, arXiv:1402.4900.
[31] A. Szorkovszky, A. A. Clerk, A. C. Doherty, and W. P. Bowen, New J. Phys. **16**, 063043 (2014).